



ELSEVIER

Contents lists available at ScienceDirect

## Applied Radiation and Isotopes

journal homepage: [www.elsevier.com/locate/apradiso](http://www.elsevier.com/locate/apradiso)Lifetime measurement of the first excited  $5/2^+$  state in  $^{133}\text{Cs}$  using NaI(Tl) and LaBr<sub>3</sub>(Ce) detectorsI.J. Lugendo<sup>a</sup>, J.K. Ahn<sup>b,\*</sup>, M.J. Kumwenda<sup>a</sup>, J.W. Lee<sup>b</sup>, B. Hong<sup>b</sup>, S.H. Hwang<sup>c</sup><sup>a</sup> Department of Physics, University of Dar Es Salaam, P.O. Box 35063, Dar Es Salaam, United Republic of Tanzania<sup>b</sup> Department of Physics, Korea University, Seoul, 02841, Republic of Korea<sup>c</sup> Korea Research Institute of Standards and Science (KRISS), Daejeon, 34113, Republic of Korea

## ARTICLE INFO

## Keywords:

Lifetime

LaBr<sub>3</sub>(Ce) scintillator

NaI(Tl) scintillator

 $^{133}\text{Cs}$ 

## ABSTRACT

We report a new high-precision lifetime measurement of the first excited  $5/2^+$  state of  $^{133}\text{Cs}$  using NaI(Tl) and LaBr<sub>3</sub>(Ce) detectors. The time difference between the coincident decays of two successive states was measured using fast-timing electronics. The 356-keV ( $1/2^+ \rightarrow 5/2^+$ ) gamma transition was tagged by the successive 81-keV ( $5/2^+ \rightarrow 7/2^+$ ) transition of  $^{133}\text{Cs}$ . The half-life of the first excited  $5/2^+$   $^{133}\text{Cs}$  state was measured as  $T_{1/2} = 6.283 \pm 0.004$  (stat.)  $\pm$  0.011(syst.) ns.

## 1. Introduction

Lifetime measurements of excited nuclear states offer one of the most stringent tests of the nuclear models. The Weisskopf single-particle transition probability can be derived from mean lifetime ( $\tau$ ) measurements using the partial gamma-lifetimes  $\tau(E\ell; M\ell)$ , where  $B(E\ell; M\ell) \propto 1/\tau(E\ell; M\ell)$  for the  $\ell$ -th electric ( $E\ell$ ) or magnetic ( $M\ell$ ) transitions.

The possible change of lifetime for certain nuclear levels has long been of interest in nuclear physics. In the early days the effects of nuclear pressure, temperature, and electron density on  $\tau$  of nuclei were intensively investigated (Bainbridge et al., 1953). Later a small change of the order of  $10^{-3} \sim 10^{-4}$  on the decay rates of  $^7\text{Be}$ ,  $^{99m}\text{Tc}$  and  $^{125m}\text{Te}$  were also observed when they were in the form of chemical compounds (Liu and Huh, 2000). More recently, the possible variation of  $\tau$  was proposed when the decayed photons are coherently reflected by environment and reabsorbed by the source nucleus (Cheon and Jeong, 2005; Cheon, 2001, 2015). However, the expected variation in  $\tau$  is very small on the order of a few %. Thus, to confirm or refute such a theoretical prediction requires the precise experimental data on the value of  $\tau$  for a given excited state of a specific isotope. Since the existing data cannot provide any firm conclusion yet, we have attempted a precise measurement of the nuclear lifetime in this research.

According to the previous work (Cheon and Jeong, 2005; Cheon, 2001), prolongation of the lifetime can most effectively be measured when the source is contained in a cylindrical metal container. The smaller radius of the reflecting container is more advantageous.

Furthermore, the change in the lifetime of a nuclear state has been reported to be larger at a lower temperature. Thus, for the purpose of this study, we have paid heed to develop an experimental setup that enables us to meet all the necessary conditions as well as precisely measuring the lifetime of the first excited state of  $^{133}\text{Cs}$ .

Excited states in  $^{133}\text{Cs}$  can be accessible through electron capture by  $^{133}\text{Ba}$ ,  $\beta$ -decay of  $^{133}\text{Xe}$ , or Coulomb excitation. The nuclear spins and parities for the ground and first excited states in  $^{133}\text{Cs}$  are assigned as  $7/2^+$  and  $5/2^+$ , respectively (Khazov et al., 2011; Blasi et al., 1967; Winn and Sarantites, 1970). The first excited state at 81 keV can be populated via the E2 transition from the 437-keV  $1/2^+$  state with  $E_\gamma = 356$  keV (See Fig. 1). The transition from the 81-keV state to the ground state is known to contain E2 and M1 admixtures.

The half-life ( $T_{1/2}$ ) of the 81-keV state has been measured using various experimental methods over the past few decades. Among them, only a few measurements reported half-life values with uncertainties below 1%. Bodenstedt et al. reported a value of  $T_{1/2} = 6.31 \pm 0.05$  ns using the  $\gamma$ - $\gamma$  coincidence measurement with NaI(Tl) detectors (Bodenstedt et al., 1959). Väilivaara et al. reported a half-life of  $T_{1/2} = 6.27 \pm 0.04$  ns measured using long-lens electron-electron spectrometers (alivaara et al., 1970). Cheon reported the half-life of the 81-keV  $^{133}\text{Cs}$  level measured to be  $T_{1/2} = 6.33 \pm 0.10$  ns using the Mössbauer method (Cheon, 2001). Mach et al. reported the half-life to be  $T_{1/2} = 6.321 \pm 0.035$  ns (Mach et al., 1989) using  $\gamma$ - $\gamma$  coincidences with two BaF<sub>2</sub> detectors, and this has been the most precise measurement so far.

The weighted average value of all previous measurement results is

\* Corresponding author.

E-mail address: [ahnjk@korea.ac.kr](mailto:ahnjk@korea.ac.kr) (J.K. Ahn).<https://doi.org/10.1016/j.apradiso.2019.05.027>

Received 9 October 2018; Received in revised form 5 April 2019; Accepted 16 May 2019

Available online 20 May 2019

0969-8043/ © 2019 Published by Elsevier Ltd.

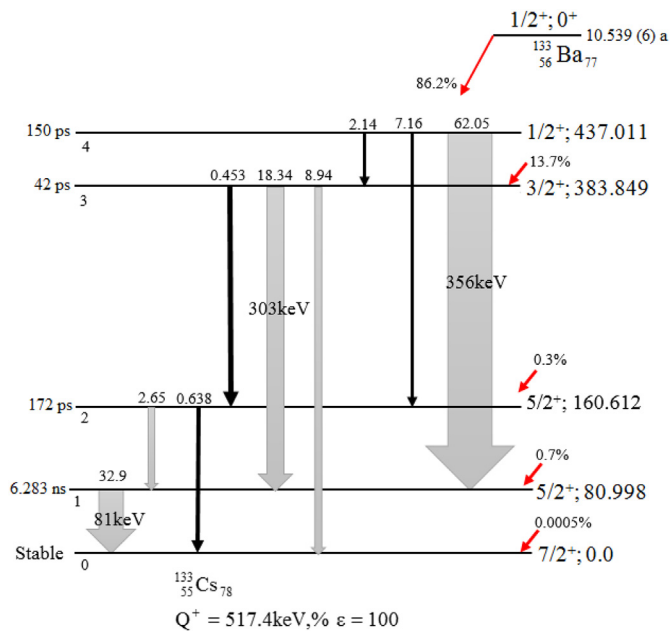


Fig. 1. Decay schemes of <sup>133</sup>Ba. The widths of arrows reflect the transition probabilities qualitatively.

quoted as  $T_{1/2} = 6.283 \pm 0.014$  ns (Khazov et al., 2011). The transition probabilities in Weisskopf units (W.u.) for the transition from the 81-keV state ( $5/2^+$ ) to the ground state ( $7/2^+$ ) in <sup>133</sup>Cs are then  $B(M1) = 0.002381 \pm 0.000022$  and  $B(E2) = 5.8 \pm 0.4$  (Khazov et al., 2011). Imanishi et al. (1967) reported that the  $B(E2\uparrow)$  value for the transition from the ground state to the 81-keV level was determined to be  $0.022 \pm 0.004 e^2b^2$  by Coulomb excitation, which can be quoted as  $7.3 \pm 1.3$  W.u. Using the relation  $B(E2)(J_b \rightarrow J_a) = (2J_a + 1)/(2J_b + 1) \cdot B(E2\uparrow)$  and  $B_W(E2) = 0.0594 \cdot A^{4/3} e^2fm^4 = 4.03 \times 10^{-3} e^2b^2$ . The half-life of the 81-keV state was also evaluated to be  $4.5^{+1.7}_{-0.9}$  ns using  $B(E2)$  values obtained by Coulomb-excitation experiments (Khazov et al., 2011).

In this paper, we report a new high-precision lifetime measurement of the first excited  $5/2^+$  <sup>133</sup>Cs state using NaI(Tl) and LaBr<sub>3</sub>(Ce) detectors.

## 2. Experiment

The fast-timing measurement system consists of two LaBr<sub>3</sub>(Ce) detectors and two NaI(Tl) detectors. The LaBr<sub>3</sub>(Ce) detectors are made of a  $1(\phi) \times 1(t)$  in crystal (labeled as D1) coupled to an 8-stage photomultiplier (XP 2060) and a  $1.5 \times 1.5$  in LaBr<sub>3</sub>(Ce) crystal (labeled as D2) coupled to a 12-stage photomultiplier (R6231). The two LaBr<sub>3</sub> detectors have an energy resolution of 2.9% for the 662-keV <sup>137</sup>Cs line and a rise time of 0.2 ns of the time signal (Derenzo et al., 2014). The NaI(Tl) detectors are made of  $2 \times 2$  in NaI(Tl) crystals (D3 and D4) coupled to 12-stage photomultipliers.

The same-crystal detector pairs were positioned to face each other. The end face of each detector was separated from the source by 6 cm. The 189-kBq <sup>133</sup>Ba radioactive source was placed at the center of the system. The source was wrapped in a 50- $\mu$ m thick polyester film and was 5 mm in diameter.

The experimental setup is schematically shown in Fig. 2. The analog signal from each of the four detectors was divided into two branches by a splitter (Phillips Scientific 740). One side was discriminated in a 16-channel leading-edge discriminator (Phillips Scientific 706) with two outputs. One output was fed into a logic coincidence module to realize a two-fold coincidence gate. The other output was digitized in a CAMAC time-to-digital converter (TDC, Phillips Scientific 7186) with a 25-ps resolution and 100-ns dynamic range. The second branch was connected to a 12-bit CAMAC analog-to-digital converter (ADC, REPIC

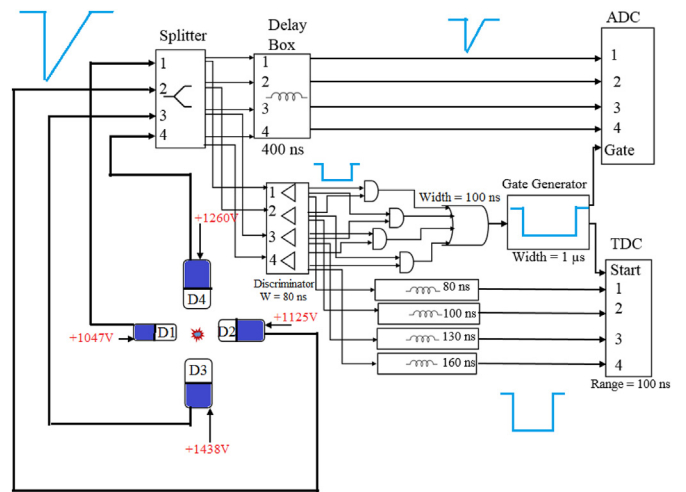


Fig. 2. Schematic view of the experimental setup and the electronics diagram.

RPC-022), gated with a 1- $\mu$ s event trigger gate. The two-fold coincidence signals from each detector pair were then OR-ed to provide both the START signal for the TDC measurement and the gate signal for the ADC measurement.

Energy calibration was performed using a least-squares fit of the seven major <sup>133</sup>Ba, <sup>137</sup>Cs, and <sup>60</sup>Co  $\gamma$ -lines of the standard sources by a quadratic curve. The energy resolutions of the LaBr<sub>3</sub>(Ce) detectors were found to vary from 3.5% for the full width at half-maximum (FWHM) at 356 keV to 5.5% at 81 keV, whereas those for NaI(Tl) detectors ranged from 8 to 10%. The  $\gamma$ -ray energy spectra of <sup>133</sup>Ba are presented in Fig. 3. Both the D2 and D4 spectra resolve the two  $\gamma$ -ray lines at 81 keV and 356 keV.

The time-walk correction for the energy range from 60 keV to 511 keV was performed using the 511 keV line from a <sup>22</sup>Na source and its Compton continuum. While one detector triggered the 511 keV line, the other changed its energy window in 30 keV intervals with the 23 keV gate width. The time variation regarding the photon energy is shown in Fig. 4 (a). The timing resolution was improved by 5% at 511 keV with the time-walk correction.

The typical  $\gamma$ - $\gamma$  timing resolutions for the LaBr<sub>3</sub>(Ce) and NaI(Tl) detectors were approximately 480-ps FWHM and 860-ps FWHM, respectively, for the 1173-keV and 1332-keV <sup>60</sup>Co lines. The time spectrum for subsequent decays in <sup>60</sup>Co was measured using the same fast-timing electronics, as shown in Fig. 4(c).

Events were collected when any of the LaBr<sub>3</sub>(Ce) or NaI(Tl) detector pairs were triggered. Approximately  $1.17 \times 10^6$   $\gamma$ - $\gamma$  coincidence events were recorded. Among them,  $4.74 \times 10^5$  events were due to a two-fold

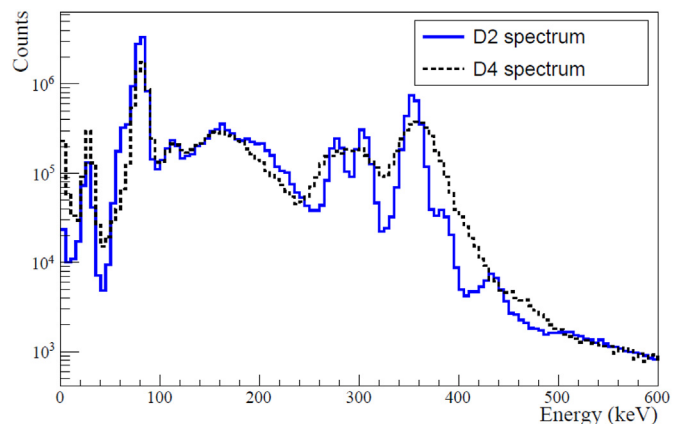
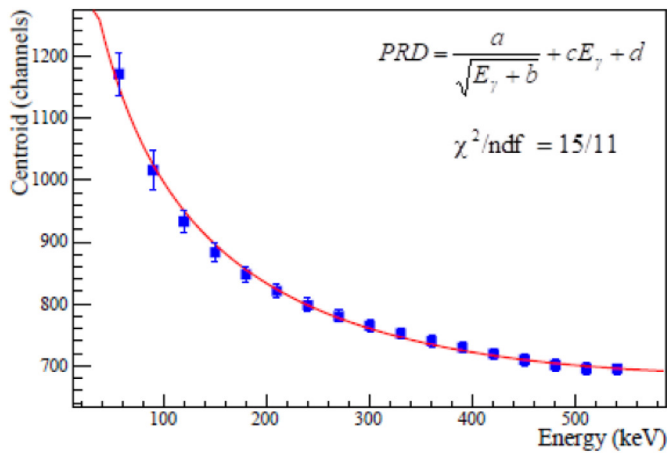
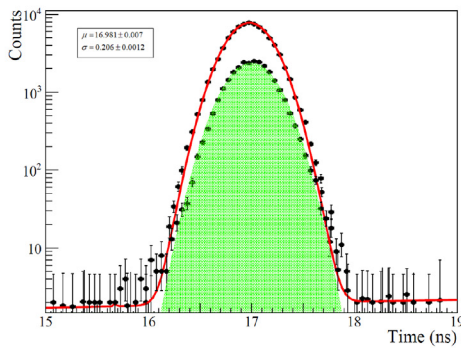


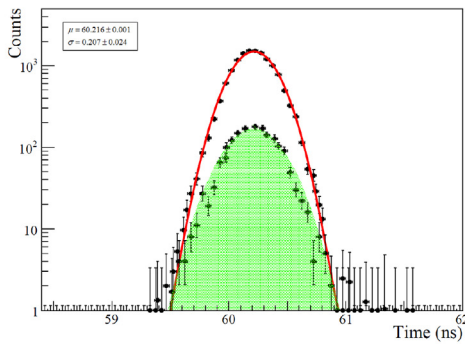
Fig. 3. Energy spectra of the  $\gamma$ -rays from <sup>133</sup>Ba measured by the D2 LaBr<sub>3</sub>(Ce) (solid) and D4 NaI(Tl) detector (dashed).



(a)



(b)



(c)

**Fig. 4.** (a) Time variations for the energy range from 60 keV to 511 keV. The time-walk effect was corrected using the overlaid least-square fit result. (b) Time spectrum for the 511-keV  $\gamma$  rays from  $^{22}\text{Na}$ . (c) Time spectrum for the 1332-keV and 1173-keV  $\gamma$  rays from  $^{60}\text{Co}$ . The filled area represents the contribution from sideband events.

coincidence with  $\text{LaBr}_3(\text{Ce})$  detectors, and  $6.99 \times 10^5$  events with  $\text{NaI}(\text{Tl})$  detectors (Lugendo, 2017).

### 3. Data analysis and experimental results

The  $\gamma$ - $\gamma$  coincidence events from  $^{133}\text{Cs}^*$  decays were measured in the energy region above 60 keV. The correlation of the two  $\gamma$ -ray energies is presented in Fig. 5. The two spots corresponding to the 356-keV and 81-keV  $\gamma$ -ray coincidence events can be seen in the scatter plot of  $\gamma$ -ray energies measured by the two  $\text{LaBr}_3(\text{Ce})$  detectors. The 356–81 keV cascade events were observed in the gating energy

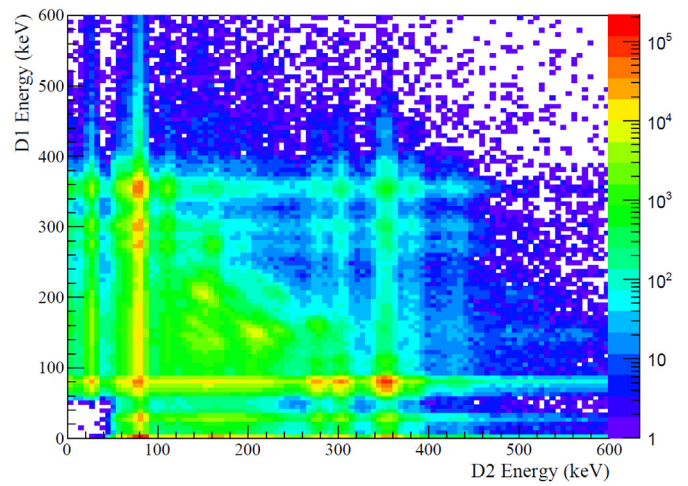


**Fig. 5.** Scatter plot of  $\gamma$ - $\gamma$  coincidence events measured by the  $\text{LaBr}_3(\text{Ce})$  detectors.

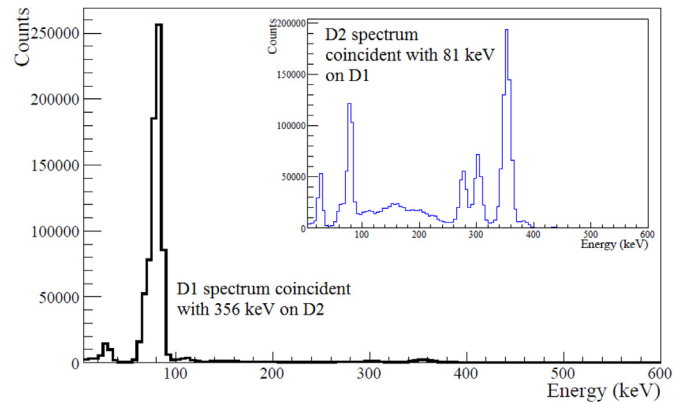


**Fig. 6.**  $\gamma$ -ray energy spectrum of D1 events gated by 356-keV events from D2.

windows of 340–400 keV for the 356-keV line and 65–85 keV for the 81-keV line.

The 356-keV gated  $\gamma$ -ray energy spectrum is shown in Fig. 6, with the 81-keV gated spectrum displayed in the inset. The 81-keV peak is observed only when the 356-keV line is gated. In the 81-keV gated  $\gamma$ -ray energy spectrum, two more peaks—at 276 keV and 303 keV—are present between the 81-keV and 356-keV peaks, which correspond to the  $\gamma$ -ray  $3/2^+ \rightarrow 5/2^+$  and  $1/2^+ \rightarrow 5/2^+$  transitions. The 81–80 keV  $\gamma$ -ray cascade through two intermediate levels with  $5/2^+$  can also be seen in the 81-keV gated spectrum. The lowest energy peak at 30.8 keV is due to Cs K-shell X-rays. The 356–81 keV  $\gamma$ -ray cascade then involves only the first excited level with  $5/2^+$  at 81 keV.

The D1  $\text{LaBr}_3(\text{Ce})$  detector was assigned to measure the delay time of the 81-keV signal, while the D2  $\text{LaBr}_3(\text{Ce})$  detector registered the starting 356-keV signal. From the  $\text{NaI}(\text{Tl})$  detectors, D3 measured the 81-keV signal, and D4 the 356-keV signal. Fig. 7 shows the raw spectrum of the time differences between the 81–356 keV signals from the two  $\text{LaBr}_3(\text{Ce})$  detectors. Events in the sideband regions were also selected to study lifetime dependence from background events. The sideband regions correspond to 10-keV wide energy regions above the signal window.

Fig. 8 represents the lifetime spectra of the 81-keV excited  $^{133}\text{Cs}$  state measured with four pair combinations of the  $\text{LaBr}_3(\text{Ce})$  and  $\text{NaI}(\text{Tl})$  detectors. The lifetime distribution was fitted with the convolution of the Gaussian prompt response function (PRF) and the exponential decay function expressed as

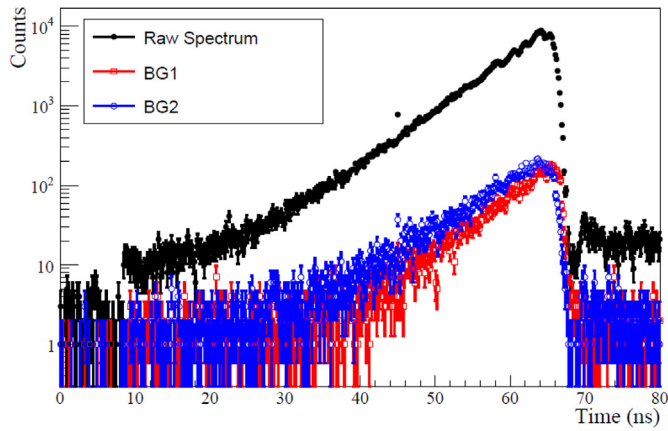


Fig. 7. Raw spectrum of time differences between the 81-keV and 356-keV  $\gamma$  rays. The filled circles represent the measured data, while the open circles and squares correspond to the events in the two sideband regions.

$$F(t) = \frac{N_0}{\tau} \int_{-\infty}^t P(t' - t_0) e^{-\lambda(t-t')} dt', \quad (1)$$

where  $N_0$  is the total number of detected  $\gamma$ - $\gamma$  coincidence events.  $\tau$  denotes the mean lifetime of a nuclear excited state populated by the

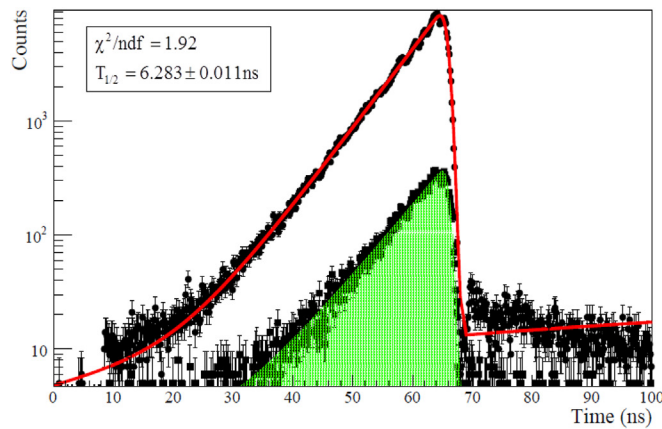
Table 1

Systematic uncertainties of the lifetime measurement of the  $5/2^+$  first excited  $^{133}\text{Cs}$  state. The total uncertainty was calculated by adding the individual contributions in quadrature.

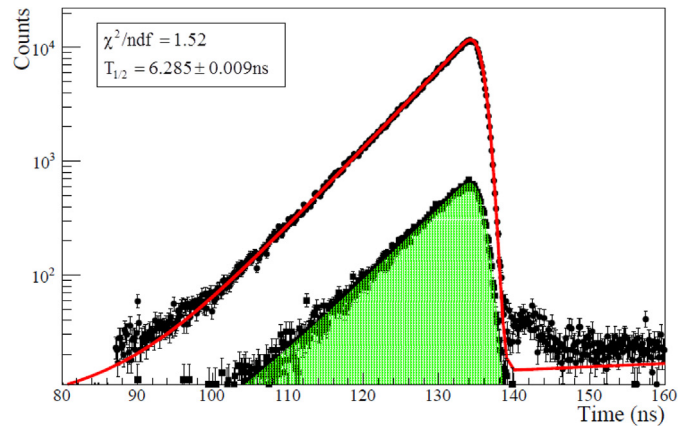
Uncertainty Component	$\sigma(T_{1/2})$ (ps)
Prompt Peak Width	6.8
Background Effect	6.4
Prompt Response Function	6.0
Coincidence Resolution	1.7
Total	11.2

selected  $\gamma$ - $\gamma$  cascade, and  $t_0$  is the centroid of the PRF peak. The standard deviation of the PRF distribution was fixed to the value obtained from the time measurement with two  $\gamma$  cascade  $^{60}\text{Co}$  lines. As a cross-check, the fit was performed with a variable resolution parameter. No deviation from the default lifetime measurement was observed. Both the signal and background distributions are assumed as the convolution functions. The lifetime distribution is then evaluated using a log-likelihood fit. The half-life ( $T_{1/2}$ ) of the 81-keV excited  $^{133}\text{Cs}$  state was deduced as  $6.283 \pm 0.010$  ns.

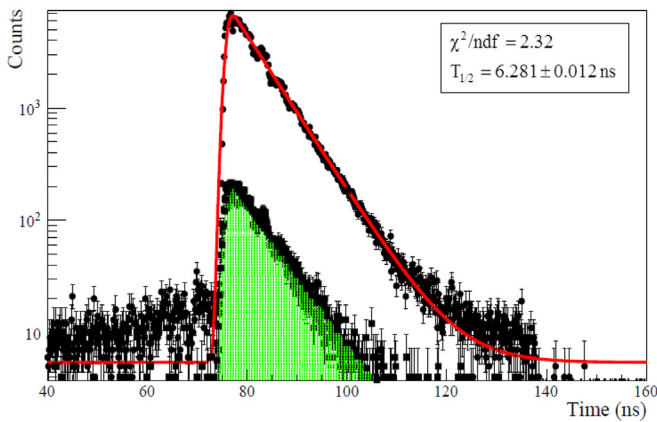
A wide range of systematic effects that can influence the lifetime measurement has been evaluated. Their individual contributions to the systematic uncertainties are described below and the deduced values



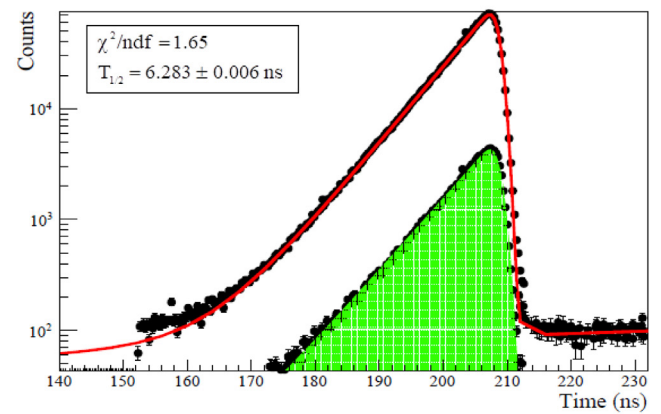
(a)



(b)



(c)



(d)

Fig. 8. Time spectra of the 81-keV  $^{133}\text{Cs}$  state coincident with the 356-keV  $\gamma$  ray that include four combination orders of the LaBr<sub>3</sub>(Ce) and NaI(Tl) detectors: (a) D1 (81-keV) and D2 (356-keV), (b) D1 (81-keV) and D3 (356-keV), (c) D2 (81-keV) and D1 (356-keV), and (d) D2 (81-keV) and D4 (356-keV). Circles represent the events in the signal window, whereas squares denote the background events estimated from the sideband analysis. Red lines are the results of the fit by the convolution function. Green areas are the results of the fit of the background events. (For interpretation of the references to colour in this figure legend, the reader is referred to the Web version of this article.)

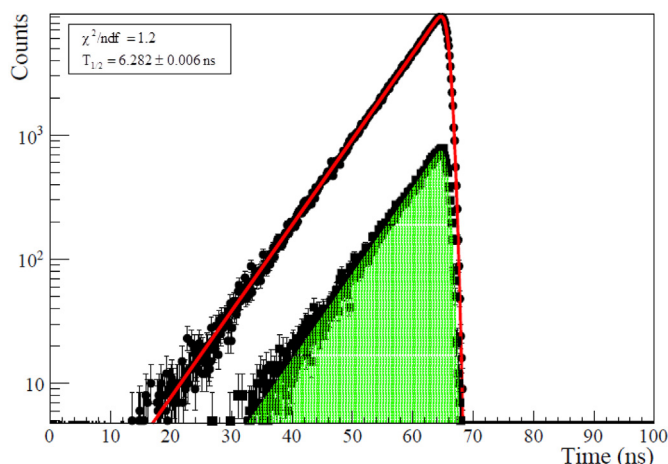


Fig. 9. Simulated spectrum of time differences between the 81-keV and 356-keV  $\gamma$  rays. The filled circles represent the signal events, while the squares correspond to the events in the two sideband regions.

listed in Table 1. Their deduced values are listed in Table 1. These systematic effects include uncertainties in the intrinsic timing resolution of the measurement system, the background contamination in the signal window, the PRF function estimation, and accidental coincidences.

The systematic uncertainty in the intrinsic timing resolution accounts for a variation in the spread of the time spectra of the 1332-keV and 1173-keV  $\gamma$ -rays from  $^{60}\text{Co}$ . The averaged uncertainties of the widths of the time spectra for every detector combination are taken as the systematic uncertainty in the timing resolution, which was deduced to be 6.8 ps.

To deduce the uncertainties caused by background events beneath the  $\gamma$ - $\gamma$  coincidence signal, two high-energy sideband regions, and their overlap region were selected. Subtracting the events in the overlap region from the events in the two sidebands, the lifetime was measured for exclusive background events in the latter. The background time spectrum was then generated by a Monte-Carlo simulation to fit the number of background events in the signal region. Finally, it was subtracted from the time spectrum in the signal region. The background subtraction was also tested with simulated signal events for all detector combinations, as shown in Fig. 9. The uncertainty due to the background contribution was evaluated to be 6.4 ps.

The drift of the PRF peak position was also considered as a possible contribution to the systematic uncertainties of the lifetime measurement. During a long-term measurement, the drift of the PRF peak position was monitored every 5 h. The convolution functions were then tailored with the assigned peak values varying in the  $1\text{-}\sigma$  interval of the peak position distributions. The drift of the PRF peak was found to account for a systematic uncertainty of 6.0 ps.

There could be accidental coincidence events present originating from two  $\gamma$ s from decays of different nuclei. Assuming random and independent decays of these two nuclei, the accidental coincidence ratio can be calculated as  $N_{\text{acc}}/N_{\text{true}} = 2A\Delta T$ , where  $N_{\text{true}}$  is the number of true coincidence events, while  $N_{\text{acc}}$  is the number of accidental coincidence events. A source radioactivity is quoted as  $A$ , and the term  $\Delta T$  denotes the 100-ns width of the  $\gamma$ - $\gamma$  coincidence time gate. Based on the probability of observing accidental coincidence events, 0.037,

accidental coincidence events were generated to reproduce the measured time spectra. The variation in the number of accidental coincidence events yielded a systematic uncertainty of the lifetime measurement of 1.7 ps.

The combined statistical uncertainty  $\sigma_{\text{tot}}$  with four combinations of detector pairs was deduced to be 4.3 ps. The measured half-life of  $5/2^+$  first excited  $^{133}\text{Cs}$  state was deduced as  $T_{1/2} = 6.283 \pm 0.007(\text{stat.}) (\text{syst.})$  ns, which is in good agreement with the world-average value (Khazov et al., 2011). The half-life reported in this study is the most precise value ever made. It should be noted that this  $\gamma$ - $\gamma$  coincidence measurement provides higher statistical precision than the previous measurement reported by Mach et al. (1989) because of more precise tagging of the 81-keV  $\gamma$ -ray line.

#### 4. Summary

We report a new high-precision lifetime measurement of the first excited  $5/2^+$   $^{133}\text{Cs}$  state using NaI(Tl) and LaBr<sub>3</sub>(Ce) detectors. The time difference between coincident photons from two successive states was measured by fast-timing electronics. The 356-keV ( $1/2^+ \rightarrow 5/2^+$ ) gamma transition was tagged with the successive 81-keV ( $5/2^+ \rightarrow 7/2^+$ ) transition of  $^{133}\text{Cs}$ . Systematic uncertainties of the half-life measurements were thoroughly studied using a Monte Carlo simulation. The half-life of the first excited  $5/2^+$   $^{133}\text{Cs}$  state was measured as  $T_{1/2} = 6.283 \pm 0.004(\text{stat.}) (\text{syst.})$  ns.

#### Acknowledgment

We are greatly indebted to J.M. Lee at KRISS for providing a  $^{133}\text{Ba}$  radioactive source encapsulated in a thin film. This work was supported in part by the National Research Foundation of Korea and Korea University.

#### References

- alivaara, K.G., Marelius, A., Kozyczkowski, J., 1970. Transition probabilities of excited nuclear states in  $^{133}\text{Cs}$ . *Phys. Scripta* 2, 19–22.
- Bainbridge, K.T., Goldhaber, M., Wilson, E., 1953. Influence of the chemical state on the lifetime of a nuclear isomer,  $^{99\text{m}}\text{Tm}$ . *Phys. Rev.* 90, 430–439.
- Blasi, P., Bocciaolini, M., Maurenzig, P.R., Sona, P., Taccetti, N., 1967. The decay of  $^{133}\text{Ba}$  and nuclear transitions in  $^{133}\text{Cs}$ . *Il Nuovo Cimento B* 2, 298–308.
- Bodenstedt, E., Korner, H.J., Matthias, E., 1959. Angular correlation measurements on  $^{133}\text{Cs}$  and the magnetic moment of the 81 keV-level. *Nucl. Phys.* 11, 584–598.
- Cheon, I.-T., 2001. Measurement of the width of the first excited state in  $^{133}\text{Cs}$ . *J. Phys. Soc. Jpn.* 70 (11), 3193–3196.
- Cheon, I.-T., 2015. Physics behind modification of the nuclear lifetime by the  $\gamma$ -ray boomerang effect. *Phys. Sci. Int. Journal* 5 (1), 12–17.
- Cheon, I.-T., Jeong, M.T., 2005. Measurement of the nuclear lifetime altered by two parallel plates. *J. Korean Phys. Soc.* 46 (2), 397–400.
- Derenzo, S.E., Choong, W.-S., Moses, W.W., 2014. Fundamental limits of scintillation detector timing precision. *Phys. Med. Biol.* 59, 3261–3286.
- Imanishi, N., Fukuzawa, F., Sakisaka, M., Uemura, Y., 1967. Coulomb excitation of  $^{45}\text{Sc}$ ,  $^{75}\text{As}$ ,  $^{127}\text{I}$  and  $^{133}\text{Cs}$ . *Nucl. Phys.* 101, 654–662.
- Khazov, Yu, Rodionov, A., Kondev, F.G., 2011. Nuclear data sheets for  $A = 133$ . *Nucl. Data Sheets* 112 (4), 855–1113.
- Liu, L.-G., Huh, C.-A., 2000. Effect of pressure on the decay rate of  $^7\text{Be}$ . *Earth Planet. Sci. Lett.* 180, 163–167.
- Lugendo, I., 2017. Possible Change in Lifetime of the First Excited State of  $^{133}\text{Cs}$  in a Metal Reflector at Low Temperature. Ph.D dissertation. Korea University.
- Mach, H., Gill, R.L., Moszynski, M., 1989. A method for picosecond lifetime measurements for neutron-rich nuclei(1) outline of the method. *Nucl. Instrum. Methods Phys. Res. Sect. A Accel. Spectrom. Detect. Assoc. Equip.* 280, 49–72.
- Winn, W.G., Sarantites, D.G., 1970.  $\gamma$ - $\gamma$  directional correlations in  $^{133}\text{Cs}$  via Ge(Li)-Ge(Li) measurement. *Phys. Rev. C* 1 (1), 215–228.